Heliyon xxx (xxxx) xxx

Contents lists available at ScienceDirect

Heliyon

journal homepage: www.cell.com/heliyon

Research article

Kinetics of thermal degradation and lifetime study of poly(vinylidene fluoride) (PVDF) subjected to bioethanol fuel accelerated aging

Agmar José de Jesus Silva *, Maria Marjorie Contreras, Christine Rabello Nascimento, Marysilvia Ferreira da Costa

Programa de Engenharia Metalúrgica e de Materiais – PEMM/COPPE/UFRJ, Universidade Federal do Rio de Janeiro, Rio de Janeiro 68525, Brazil

ARTICLE INFO

Keywords:
Materials science
Materials chemistry
Poly(vinylidene fluoride)
Aging
Bioethanol fuel
Kinetics analysis
Activation energy
Lifetime prediction

ABSTRACT

PVDF was prepared by compression molding, and its phase content/structure was assessed by WAXD, DSC, and FTIR-ATR spectroscopy. Next, PVDF samples were aged in bioethanol fuel at 60 °C or annealed in the same temperature by 30 — 180 days. Then, the influence of aging/annealing on thermal stability, thermal degradation kinetics, and lifetime of the PVDF was investigated by thermogravimetric analysis (TGA/DTG), as well as the structure was again examined. The crystallinity of ~41% (from WAXD) or ~49% (from DSC) were identified for unaged PVDF, without significant changes after aging or annealing. This PVDF presented not only one phase, but a mixture of α-, β- and γ-phases, α- and β-phases with more highlighted vibrational bands. Thermal degradation kinetics was evaluated using the non-isothermal Ozawa–Flynn–Wall method. The activation energy (E_a) of thermal degradation was calculated for conversion levels of $\alpha = 5 - 50\%$ at constant heating rates (5, 10, 20, and 40 °C min^{-1}), $\alpha = 10\%$ was fixed for lifetime estimation. The results indicated that temperature alone does not affect the material, but its combination with bioethanol reduced the onset temperature and E_a of primary thermal degradation. Additionally, the material lifetime decreased until about five decades ($T_f = 25$ °C and 90 days of exposition) due to the fluid effect after aging.

1. Introduction

Thermoplastic polymers, even those specials such as the engineering polymers, experience aging during its operating lifetime. Polymer aging is a time-dependent process that may have physical and/or chemical origins [1, 2, 3, 4, 5]. Chemical aging involves chemical changes, e.g., chain scission, crosslinking, and oxidative reactions, which may modify the polymer molecular weight distribution. Physical aging occurs alongside the other forms of aging without involving reactions and chemical changes; however, physical characteristics such as density, crystallinity, and color can be modified [3, 4]. Due to the high complexity of aging processes, combinations of two or more effects are usually observed [4], and changes in mechanical, thermal, and thermomechanical properties may occur [4, 5, 6, 7]. Moreover, the aging process is susceptible to variables such as temperature, mechanical stress, and chemical aggressiveness of the environment [5, 6, 7].

Poly(vinylidene fluoride) (PVDF) is an engineering thermoplastic polymer widely used in the specific plastic sectors [7, 8, 9, 10]. The nonpolar α-form PVDF has its use well consolidated in structural applications such as flexible pipes for oil and gas exploration [11, 12, 13, 14]. PVDF can also be employed as a liner (coating) or inner layer in multilayers thermoplastic pipes or storage tanks dedicated to storage and/or transportation of biofuels, mixtures of biofuels-gasoline and sodium hydroxide solutions (except in critical conditions, i.e., temperature range from 50 to 90 °C and pH of 13.5–14), among others [5, 7, 13, 15, 16, 17, 18, 19, 20]. Additionally, PVDF has several other industrial uses, including valves, membrane filters, pumps and bearings, chemicals and pharmaceuticals packaging, and barrier for gaseous substances [7, 8, 19, 21]. All these applications are possible due to PVDF chemical inertness, associated with an outstanding mechanical performance and weatherability even in aggressive environments and under high temperatures [19].

Biofuels such as bioethanol are currently a promising and sustainable alternative in the worldwide energy system production. Besides being competitive with fossil fuels, biofuels are produced from renewable raw sources and are less aggressive for the environment. Bioenergy sources are diverse, e.g., bioethanol from sugarcane has been widely produced in Brazil, but soybean, corn, and beets may alternatively be used. After

* Corresponding author.
E-mail address: agmarster@gmail.com (A.J. de Jesus Silva).

https://doi.org/10.1016/j.heliyon.2020.e04573
Received 20 December 2019; Received in revised form 17 March 2020; Accepted 24 July 2020

production, bioethanol needs to be safely transported to consume centers and stored. Thus, it is crucial to use storage and transportation structures compatible with the fluid, avoiding contamination due to oxidative and/or degradation processes [15]. Therefore, the knowledge of how the materials employed in such structures respond to the service conditions is a fundamental question still not thoroughly explored in the literature. For instance, when polymeric materials are employed, aging effects may emerge influencing the performance at long-time operation. A previous study performed in our research group [7] employed dynamic mechanical thermal analysis (DMTA) and time-temperature superposition principle – TTS (WLF methodology) to evaluate the long-term behavior of the PVDF aged in biofuel. It was found that some relaxations processes are modified and accelerated when aging takes place under temperature and fluid combination mainly at temperatures above *Tg*, between around – 40 and 50 °C [7].

It has been discussed that an advantageous manner to supervise changes in materials performance due to the action of aging processes is the use of thermal methods, e.g., TGA (thermogravimetric analysis), DSC (differential scanning calorimetry) and DMTA (dynamic mechanical thermal analysis) [4, 7, 15]. Among these methods, DMTA is very suitable for long-term mechanical behavior evaluation [7], while TGA and DSC are appropriately applied to perform kinetics studies and thermal lifetime estimation [6, 22, 23, 24, 25, 26, 27, 28].

In this scope, the application of TGA with multiple heating rates to evaluate polymer's degradation kinetics, as well as to estimate operating lifetime, is a particularly robust and useful thermal methodology that has been widely used [6, 22, 23, 24, 25, 26, 27, 28, 29]. Among the materials that can be evaluated are polymers and biopolymers, composites, and other organic materials that decompose in first-order kinetics [22, 23, 24, 25, 26, 27, 28, 29]. For those others that do not, the main stage of decomposition can be treated as a first-order kinetics process with good approximation.

Some investigations regarding the thermal degradation behavior of PVDF were identified [23, 24, 29, 30, 31, 32]. Nonetheless, if specific service use conditions are considered (e.g., a polymer in direct contact with fluids such as gasoline, bioethanol, biodiesels, mixtures of bioethanol/gasoline, among others), a lack of extensive studies are identified. In this sense, the purpose of this work was to complement previous findings [7] that showed interaction between fluid/-polymer/temperature and its effect on the thermomechanical behavior of PVDF. Then, it was investigated how the aging in bioethanol affects the thermal degradation kinetics, and lifetime (thermal endurance curves) of PVDF before and after its direct exposition to bioethanol fuel using the isoconversional integral method of Ozawa-Flynn-Wall (OFW model) to calculate the activation energy (E_a) of thermal degradation calculated for conversion levels of $\alpha = 5 - 50\%$ at constant heating rates (5–40 °C min^{-1}), $\alpha = 10\%$ fixed for lifetime estimation.

Once temperatures lower than 60 °C are expected during fluid/polymer contact in practical applications, an accelerated aging was categorized. Due to the relevance of thermally-induced effects, simple annealing experiments in the same temperature of aging in bioethanol were also carried. Since the polarity of the crystalline phases can affect the fluid compatibility with the polymeric structure, the knowledge of the behavior of phases was decisive to better understanding how the aging in bioethanol or annealing could interfere in the thermal stability, thermal degradation kinetics and lifetime of the PVDF in question. Hence, in this work, in a first step, a careful evaluation of structure and phase content of the material was performed through WAXD, DSC, and FTIR-ATR spectroscopy for stages before and after aging/annealing applied to the PVDF.

2. Experimental section

2.1. Polymer processing and aging

PVDF Solef® 6010 (homopolymer) fabricated by Solvay SA was used. This polymer was supplied in pellets and processed by compression molding using a rectangular stainless-steel mold (170 × 170 × 3 mm). The molding was carried in two steps; first, after a pre-heating of the polymer granules at 150 °C for 20 min, melting was performed in a hydraulic press under 6 tons pressure at 220 °C for 5 min. In a second step, the mold containing the molten polymer was cooled at 80 °C for 10 min, and subsequently more 5 min at room temperature and 0.5 ton before extraction. This process yielded plane plates with good homogeneity. Although this process route indicated a significant percentage of α-phase for the final solid-state material, some percentage of β- and γ-phases were also favored, as discussed posteriorly.

The PVDF plates were machined to prepare specimens (bars) with dimensions of 30 × 25 × 3 mm. PVDF aging experiments were carried out in commercial bioethanol fuel derived of sugarcane (hydrated ethanol 94% v/v, supplied by CENPES/Petrobras SA) over 30—180 days, producing samples for tests of DSC, WAXD and FTIR-ATR, while for TGA/DTG analyzes, the aging covered only 30—90 days due to an experimental limitation. For promoting the aging in bioethanol, PVDF samples were placed inside of glass vessels of 1 L, which were lodged in thermal baths kept at a temperature of 60 °C. On the other hand, the annealing experiments were conducted in a hot air oven under the same temperature and times used to age in bioethanol. All these experiments were conducted according to procedures established in ISO 175 standard [33]. Before aging, the as processed PVDF samples were white (opaque). After aging in bioethanol, they were yellowish, and there was a tendency of intensifying the color as aging time increased.

2.2. Characterization of crystalline phases and structure

Fourier Transform Infrared Spectroscopy with Attenuated Total Reflectance Technique (FTIR-ATR) was used to evaluate the crystalline phase content of PVDF. The FTIR-ATR spectra (in transmittance mode) were carried using a Spectrum 100 (PerkinElmer Co.) operating in the range of 4000 — 650 cm^{-1} with resolution of 4 cm^{-1}.

The crystalline structure (diffraction planes), as well as the degree of crystallinity (X_c, %) were assessed by Wide Angle X-ray Diffraction (WAXD), using a Shimadzu diffractometer operated with CuKα radiation ($\lambda = 0.1542$ nm) for 2θ values from 5 to 65°. X_c was obtained according to well-established procedures [34].

The crystallinity was also evaluated by DSC analysis. DSC curves were obtained in a Q 8000 equipment (PerkinElmer Co.) under N_2 atmosphere, applying two heating and cooling cycles, in temperature range of 25–200 °C at a rate of 10 °C min^{-1}. For this case, (X_c, %) was obtained from the melting enthalpy (ΔH_m) of the samples, which were divided by ΔH_0 (enthalpy of fusion of 100% crystalline polymer, 104.7 J g^{-1}) [35, 36].

2.3. Thermogravimetric analysis (TGA)

Non-isothermal thermogravimetric analysis (TGA), as well as the corresponding differential thermogravimetric analysis (DTG) of PVDF, before and after aging in bioethanol and annealing, were performed in a TA Q500 equipment (TA Instruments Co.), using samples of 10 mg and under N_2 atmosphere supplied at a flow rate of 60 mL min^{-1}. All samples were subject to heating rates of 5, 10, 20, and 40 °C min^{-1}, between 25 up to 700 °C to evaluate thermal stability, degradation kinetics, and

lifetime of PVDF samples. TGA analyzes and, subsequently, the calculus needed for the evaluation of the kinetics of thermal degradation and lifetime were conducted according to ASTM E1641 [37] and ASTM E1877 [38], which contain the necessary mathematical procedures used in the determination of activation energy and lifetime. The main theoretical concepts adopted from these standards, which have been discussed and applied in different experimental situations [6, 39, 40, 41], are briefly described below.

2.4. Theoretical background

There are currently several mathematical models to evaluate kinetics parameters of thermal degradation data extracted from the TGA analysis of polymers [6, 22, 39, 40, 41, 42, 43, 44]. Among them, one of the most successful is the isoconversional integral method of Ozawa-Flynn-Wall, known as OFW [22, 23, 24, 26, 27, 28, 29]. This model is a free-kinetics model since it considers that the rate constant of the degradation process at a constant degree of conversion (α) depends only on the temperature, i.e., the model-free does not depend on the reaction model, $f(\alpha)$ [39, 40, 41, 45]. In general, kinetics methods consider that solid-state reactions, which occur during thermal degradation, are governed by a single process based on Eq. (1), where $d\alpha/dt$ is the conversion rate, $f(\alpha)$ is the reaction model, α is the degree of conversion during the degradation reaction, $k(T)$ is the temperature-dependent rate constant, and T is the absolute temperature (K) [46, 47].

$$\frac{d\alpha}{dt} = k(T)f(\alpha) \tag{1}$$

The function $k(T)$ changes with temperature according to the Arrhenius equation (Eq. (2)), where A is the pre-exponential factor (s^{-1}), and E_a is the activation energy (kJ mol^{-1}) [46, 47].

$$k(T) = A\exp\left(-\frac{E_a}{RT}\right) \tag{2}$$

When the temperature increases at a constant heating rate ($\beta = dT/dt$), the function $f(\alpha)$ assumes the form defined in Eq. (3) [46, 47]. This equation is the differential conversion expression of a kinetics model function for a solid-state reaction during the degradation process, which is dependent on a specific reaction mechanism.

$$\frac{d\alpha}{dT} = \frac{A}{\beta}\exp\left(-\frac{E_a}{RT}\right)f(\alpha) \tag{3}$$

After rearrangement, Eq. (3) may lead to the integral expressed in Eq. (4), which can be solved using Doyle approximation, according to the method developed by Ozawa-Flynn-Wall [39, 40, 41]. Through this method, the activation energy can be readily determined for a given degree of conversion α, without knowledge of the reaction mechanism. Thus, the OFW method may be written as follows (Eq. (5)) [26, 27, 28].

$$g(\alpha) = \int_0^{\alpha}\frac{d\alpha}{f(\alpha)} = \frac{A}{\beta}\int_{T_0}^{T}\exp\left(-\frac{E_a}{RT}\right)dT \tag{4}$$

$$\ln\beta = -1.052\frac{E_a}{RT} + \left(\ln\frac{AE_a}{Rg(\alpha)} - 5.331\right) \tag{5}$$

According to Eq. (5), a plot of $\ln\beta$ versus $1/T$ for a constant value of α, obtained from α-T curves recorded at several heating rates (at least three), should give straight lines whose slopes allow the calculation of activation energy of the degradation process.

3. Results and discussion

3.1. Phase content and structural evaluation

WAXD and FTIR-ATR analysis were essential in the evaluation of the crystalline phase fractions of the PVDF unaged, aged in bioethanol and annealed. Since the polarity of the crystalline phases can affect the fluid compatibility with the polymeric structure, this information was decisive to understanding how the aging in bioethanol or annealing could interfere in the thermal stability, thermal degradation kinetics and lifetime. However, the identification and quantification of different PVDF phases by both techniques was difficult due to the similarities between them (shoulders and/or overlapping can occur sometimes), as also stated by [48].

The FTIR-ATR spectra of the PVDF unaged, aged in bioethanol and annealed are shown in Figure 1. The spectrum of unaged PVDF containing the typical vibration bands identified was highlighted on the right side (curve h) for better visualization and comparison. Vibration bands attributed to different PVDF phases were simultaneously observed. Based on literature reports [48, 49, 50, 51, 52], the bands at 615, 764, 794, 854 and 974 cm^{-1} identify the α-phase PVDF. On the other hand, the presence of β-phase was confirmed in the material by the well-defined vibrational bands at 1279 and 1431 cm^{-1} [50, 51, 52], both indicated by the vertical dashed lines in Figure 1. Besides, the two minor bands observed at 833 cm^{-1} and 1242 cm^{-1} are usually associated with the presence of γ-phase [48, 50], i.e., this PVDF presented a mixture of α-, β- and γ-phases, and not just one of them.

The band at 842 cm^{-1} (also indicated by a vertical dashed line in Figure 1), is doubtful, i.e., some author report it as typical of β-phase [48, 49, 51, 53, 54, 55], whereas other as common to both, γ and β-phases of PVDF [50, 54]. In the present case, we attributed this peak as indicative of PVDF β-phase because the γ-phase peaks (833 and 1242 cm—^{1}) appeared only as shoulders, while other typical γ-phase peaks (776 and 812 cm—^{1}) were absent.

No changes were observed in the vibration bands' quantity or intensities when the spectra of the PVDF aged in bioethanol or annealed were compared with the unaged one, indicating that material structure was conserved.

The presence of β-phase verified in the PVDF unaged, aged in bioethanol and annealed during the different aging times, even that numerically not quantified here, was a curious occurrence. In general, the literature reports that the α-phase is predominant in the melt-crystalized PVDF, which occurs mainly below 160 °C [48, 56, 57, 58, 59, 60]. In this work, the melted PVDF was cooled in two steps. Firstly, after melting under 6 tons pressure at 220 °C for 5 min, the mold containing the polymer was cooled at 80 °C for 10 min, and subsequently, in a second step the material was cooled at room temperature by 5 more minutes and 0.5 ton before extraction. Despite similarities in this procedure with those from the literature [48, 56, 57, 58, 59, 60], the α-phase was not exclusively yielded here. The typical β-PVDF vibration bands identified in Figure 1 are an irrefutable register that β-phase occurred simultaneously with α-phase, and also, γ-phase, this last apparently in tiny quantities.

The literature reports two well-established experimental procedures to generate polar β-phase. One of them is by crystallization from solutions of PVDF in dimethylformamide (DMF) or dimethylacetamide (DMA) in temperatures below 70 °C [56]. Alternatively, the β-phase can also be obtained by stretching of the α-phase at a rate of 10—50 cm min^{-1} [55]. Ribeiro et al. [61] described that β-films could be obtained by

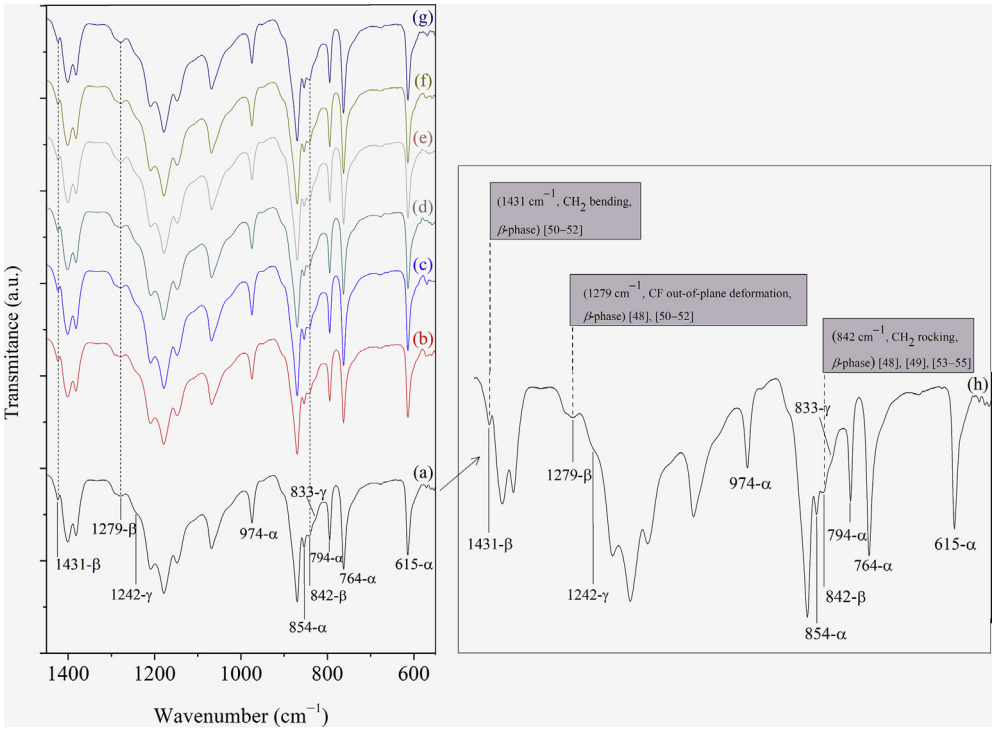

Figure 1. FTIR-ATR spectra of the PVDF in the conditions unaged (a), aged in bioethanol (30 days—b, 90 days—d and 180 days—f), and annealed (30 days—c, 90 days—e and 180 days—g). Curve h shows the highlighted spectrum of the unaged material. Adapted and improved by permission from [7] [Springer Nature, Journal of Materials Science, De Jesus-Silva et al., COPYRIGHT, 2016].

stretching α-PVDF at temperatures between 70 and 100 °C and using a stretch ratio (R) ranging between 3 and 5. The PVDF thus obtained can still be poled by corona charge method, which can promote the still highest β-phase content. In these cases, the stretching causes the alignment of polymer chains into the crystals so that all-trans planar zigzag (TTT) conformation, allowing the dipoles on the polymer chains to align normal to the direction of the applied stress [55].

On the other hand, unlike the traditional forms, Sun et al. [49] and Song et al. [62] report that some percentage of β-phase can also be obtained by crystallization from the melt state if the crystallization rates are sufficiently fast. Song et al. [62] reported in their work that high-rate quenching at lower temperatures (films were melted at 210 °C for 10 min and then immersed very quickly into the quenchant, e.g., ice or water at temperatures of 0–80 °C) resulted in the formation of β-phase microcrystals in PVDF-PMMA blends with low PMMA contents directly from their melts. Other studies relating about PVDF β-phase formation from the melt were also reported by Martins et al. [48], Hattori et al. [63], Doll and Lando [64, 65], Hattori et al. [66], Yang and Chen [67], and Oka and Koizumi [68].

In the present study, because the PVDF processing route adopted promoted the crystallization of the material from the melt state under a compression load, the α-phase crystals were expected to be preferentially generated, as occurred (higher number of vibration bands and more intense bands for α-phase were identified in Figure 1). However, the presence of β-phase was also observed, although unexpected. Other reports in the literature have β-phase formation from the melt under pressure [48, 62, 63, 64, 65, 66, 67, 68], yielding a mixture of phases, α-, β- and γ-phases.

The WAXD patterns of the PVDF aged in bioethanol, annealed, and unaged can be seen in Figure 2. According to the literature reports, the notable peaks at $2\theta = 17.8°$ (100), 18.3° (020), 26.7° (021) and 38.7° (002) are representative of α-phase [48, 49, 51]. Furthermore, if a magnifier is used in position around $2\theta = 20°$, it can be seen the coexistence of two peaks at $2\theta = 19.9°$ and $2\theta = 20.06°$. The first of them is also relative to α-phase and associated with the diffraction plane (110) [48, 49, 55], while the peak at $2\theta = 20.06°$ is doubtful due to the proximity with the peaks of the β- and γ-phases in this region, producing divergence of opinion between authors [48, 49, 51, 53, 60]. In this work, we decide that this peak is formed by contribution of α- and β-phases (as indicated in Figure 2), with α-phase as main contributor due to the characteristics of the processing adopted (compression molding under pressure). In addition, β-phase in this material was indeed confirmed by peak at 35.8°, which exclusively identity the (001) diffraction plane of β-phase, as reported by Sun et al. [49] and Mohammadi et al. [55].

By evaluation of Figure 2 diffractograms, it can be concluded that, as occurred for FTIR-ATR analysis, the material structure was conserved after aging or annealing of this PVDF in the established conditions.

Table 1 shows the degrees of crystallinity (X_c, %) of the PVDF unaged and after aging in bioethanol or annealing, as calculated from WAXD and DSC analyses. As shown, the aged or unaged materials have X_c from WAXD lower than by DSC. According to the literature [7, 59], this difference is due to the total endotherm area of DSC, which corresponds to the sum of energy required to melt of both, crystalline and crystal-amorphous interphase regions, thus increasing the enthalpy of X_c calculation from DSC.

The most important at this point is to note that, despite the differences in the numerical values, DSC or WAXD indicate similar tendencies on increasing crystallinity degree during both, aging in bioethanol or annealing. Meanwhile, it can be seen that increasing tendency after annealing was still slightly higher than those from aging in bioethanol. For instance, from WAXD measurements after 180 days, X_c changed from ~41 to 44% and of ~41–45% after aging in bioethanol and annealing, respectively. DSC identified an analogous behavior, i.e., X_c changed from ~49 to 50% and of ~49–53% after aging in bioethanol and annealing, respectively. It is believed that these changes probably occurred due to a temperature effect, which can promote increases in crystal perfection or size, as also reported by Castagnet and Girard [69].

Finally, the results of FTIR-ATR and WAXD suggested that the obtaining of a single-phase PVDF may not be a simple procedure. Martins et al. [48] and Wang et al. [70] have pointed that the different phase

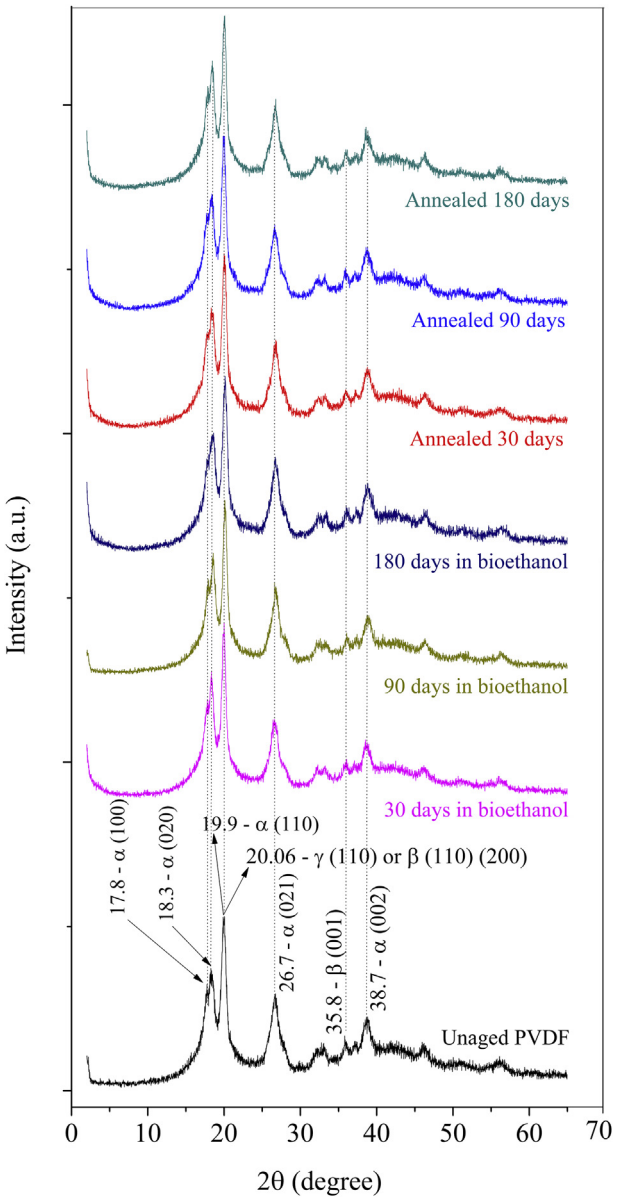

Figure 2. WAXD patterns of the PVDF unaged, aged in bioethanol and annealed during different experimental times. Adapted and improved by permission from [7] [Springer Nature, Journal of Materials Science, De Jesus-Silva et al., COPYRIGHT, 2016].

formations are defined not only by the processing conditions but also by the intrinsic semi-crystalline nature of the polymer. In this way, it can be concluded that yielding one phase in particular of this material requires additional care during the choice of the experimental technique of processing and thermal and/or superficial treatments that will be applied. Also, the efforts of more than one characterization technique are essential for a complete and decisive determination of the phase content and structure of the material.

3.2. Thermal stability

PVDF thermal stability was evaluated by comparing TGA and DTG thermograms of PVDF unaged, aged in bioethanol and annealed for times of 30 and 90 days. These thermograms are presented in Figure 3a—b (TGA) and 4a—c (DTG). Figure 3a shows that the material presented high stability up to 400 °C. Then, the thermal degradation process starts and occurs in two distinct mass-loss steps, as also reported by Mendes et al. [24] and Botelho et al. [29]. The first process, corresponding to PVDF primary degradation, occurs in the range of 400 — 510 °C (Figure 3a). The second degradation step occurs at a temperature range of 510 — 700 °C and appears as a slight slope variation compared to the first one, where the major quantity of polymer mass was lost. Once the thermograms of both thermal degradation steps undergo only minor changes after annealing, it was inferred that only thermally-induced effect was not harmful to this PVDF under the conditions employed.

The primary degradation could also be monitored by identification of onset temperatures (T_{onset}) (Table 2), i.e., temperatures at which the material effectively started the mass-loss. It can be seen that, after annealing, the onset temperatures (482 — 486 °C) were very close to the value of the unaged PVDF (485 °C), corroborating the hypothesis previously verified. Likewise, small changes were also identified in the maximum thermal decomposition peak temperatures (T_{peak}) in DTG thermograms, as shown in Figure 4a and Table 2.

On the other hand, PVDF aged in bioethanol during 30 — 90 days presented a different thermal behavior. It can be seen that after aging in bioethanol, the same two mass-loss steps described above for unaged and annealed materials appeared, as shown in Figure 3b. However, in this case, noteworthy changes in thermal stability were verified. A third and small mass-loss step was also identified at temperatures in the range of 100 — 200 °C, as shown in Figures 3b, 4b, and 4c (graph highlighted). These differences were probably related to the bioethanol acting inside of the free and constrained amorphous chains of the PVDF. As concluded recently by Silva et al. [7], PVDF absorbs bioethanol although in small amounts (1.2% at nearly 90 days of immersion, reaching saturation from there on, with a diffusion coefficient $D = 1.05 \times 10^{-9}$ cm^2 s^{-1}), in a process favored by similar polarities between fluid and polymer. Due to the hydrophobic nature of this polymer and a non-variation of mass in the temperature range (100 — 200 °C) when the unaged material is considered, the hypothesis of polymer dehydration was discarded. Hence, it is supposed that this step of mass-loss is due to a hindered evaporation process of part of the bioethanol molecules trapped inside of the free volume of PVDF amorphous chains, which occurs before the onset of the thermal degradation during melting. It is possible that the occurrence of hydrogen bonds between bioethanol and amorphous chains and/or crystals in β-phase delays the volatilization in a process analogous as reported by Li et al. [71] for water bonded in carboxymethylcellulose sodium film.

Table 1. Degrees of crystallinity (X_c) of the PVDF in stages unaged, and after aging in bioethanol fuel and post-annealing at different times of exposition. Adapted and improved from De Jesus Silva et al. [7].

Aging times	X_c – WAXD (%)	X_c – DSC (%)
Zero (unaged)	41.52 ± 0.97	48.90 ± 0.04
30 days in bioethanol	41.85 ± 0.45	49.01 ± 0.02
90 days in bioethanol	42.94 ± 0.60	48.13 ± 0.01
180 days in bioethanol	43.73 ± 0.18	50.14 ± 0.03
Annealed 30 days	42.42 ± 0.99	51.06 ± 0.02
Annealed 90 days	43.46 ± 1.10	53.86 ± 0.02
Annealed 180 days	45.24 ± 0.38	52.83 ± 0.01

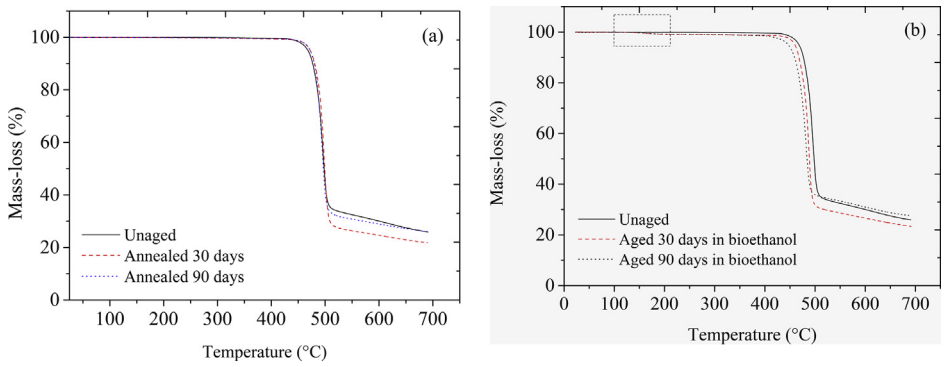

Figure 3. TGA thermograms of annealed PVDF (a), and PVDF aged in bioethanol during experimental times of 30 and 90 days (b), at 20 °C min^{-1} heating rate, compared to unaged material.

Table 2. T_{onset} and T_{peak} temperatures relatives to thermal degradation of PVDF in stages unaged, annealed and aged in bioethanol by different experimental times, extracted from TGA experiments at 20 °C min^{-1} heating rate.

Sample	T_{onset} (°C)	T_{peak} (°C)
Unaged	484.8	495.8
Annealed 30 days	486.0	497.7
Annealed 90 days	482.3	494.2
Aged 30 days in bioethanol	471.2	487.8
Aged 90 days in bioethanol	466.8	481.7

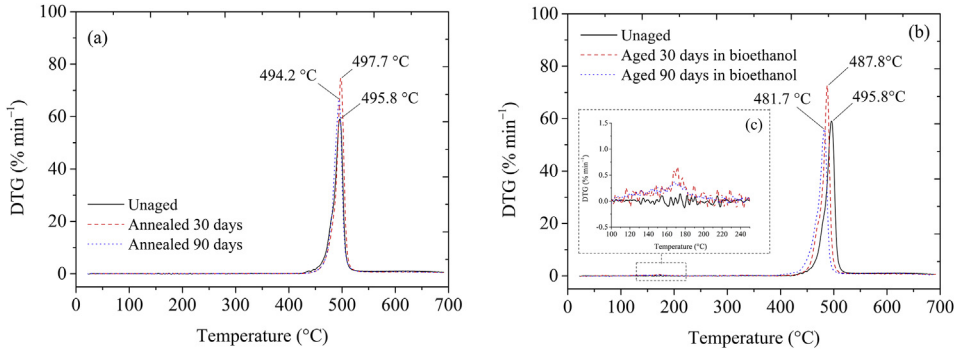

Figure 4. DTG thermograms of PVDF annealed (a), and aged in bioethanol during experimental times of 30 and 90 days (b), at 20 °C min^{-1} heating rate, compared to the unaged material. Highlight of DTG at mass-loss range of 100–200 °C (c).

Furthermore, Figure 3b shows that the onset temperatures of the PVDF aged in bioethanol during 30 and 90 days tended to decrease, and consequently thermal stability of these samples changed towards lower limits. In this case, the T_{onset} of the materials aged in bioethanol reached 467 — 471 °C, as shown in Table 2, equivalent to reductions of 2.8 — 3.7%. For this situation, changes were also found in the peak temperature of the maximum thermal degradation (Figure 4b), which changes of 496 to 488 °C and 482 °C, after 30 and 90 days of aging, respectively, corresponding to decreases of 1.6 and 2.8%, meaning that the material aged in bioethanol reached the maximum degradation rate slightly quicker than the unaged one. Although the percent changes are small, these results were indicative that bioethanol molecules volatilization outward the polymer can create favorable conditions to degradation mechanism, as it will be discussed further on. These conclusions were corroborated by comparing the activation energy profiles of the material before and after aging and annealing experiments, as it is presented in the following subsection. The changes observed were minor since the experimental conditions employed in this work were quite mild; however, it indicated the interaction of polymer and fluid. Long-term use may suffer the effect of this interaction, as it will be shown later.

Figure 3a—b shows that independent of the changes in the thermal stability of PVDF after aging in bioethanol, TGA thermograms of all the samples indicated small differences in the residual mass. As seen in Figure 3a—b, the unaged material presented 26% of the residual mass, which remained approximately equal after aging or annealing. A very close value of residual mass for PVDF was reported by Mendes et al. [23]. These results suggest that, although the thermal degradation process of PVDF after aging in bioethanol seems to change during heating, this effect did not cause modifications in the residual polymer mass.

Despite this, changes related to T_{onset} and T_{peak} temperatures of PVDF aged in bioethanol indicated a possible interaction between this fluid and the polymer structure, and a thorough evaluation of thermal degradation kinetics was carried out to determine the activation energy profiles of the thermal degradation of PVDF before and after aging in bioethanol and annealing for different conversion levels.

3.3. Thermal degradation kinetics

The activation energy profile of PVDF at the different conditions was evaluated, aiming to better understanding how the fluid affects the

thermal stability and thermal degradation kinetics of this polymer. This evaluation was complementary to the results of the long-term evaluation using thermomechanical data and carried by our group in [7]. To base the discussion, the primary mechanisms of PVDF thermal degradation were briefly revised.

Vinylidene polymers, such as PVDF, exhibit two competitive thermal degradation process, being one of them the mechanism started by carbon-hydrogen scission, which is followed by H–X elimination [29, 30, 31, 72]. The alternative process is originated from the backbone scission with the formation of halogenated or oxygenated compounds [29, 30, 31]. In the first route, due to the lower bonding strength of C–H (410 kJ mol^{-1}) compared with C–F (486 kJ mol^{-1}) [4], it is supposed that C–H scissions primarily occurs, leading to the formation of $-CH_2CF_2CH_2CF_2\dot{C}HCF_2CH_2-$ radical specimens [29, 30]. Subsequently, the presence of both hydrogen and fluorine atoms results in hydrogen fluoride (H–F) and diene specimens of type $-CH_2CF_2CH_2CF=CHCF_2CH_2CF_2-$ as degradation products [30]. This first liberation of H–F is a process favored by head to tail (H–T) defects in the molecules, which form a carbon-carbon double bond unzipping H–F molecules down the polymer chain, leading to the main degradation process [23, 29]. The further loss of H–F along with the polymer chain results in polyenic sequences of the type $-CH_2CF_2CH=CFCH=CFCH_2CF_2-$, with additional liberation of H–F [29]. Because the polyenic sequences are unstable, when the degradation temperature is increased at about 500 — 600 °C, the macromolecules undergo further complex reactions, e.g., polyaromatization [30, 31], as it is reproduced in the scheme in Figure 5. The evidence of compounds containing aromatic structures was confirmed by analyses conducted by Montaudo et al. [31] and O′ shea et al. [32]. Besides, if PVDF is synthesized from the persulfate initiator (emulsion process) [19, 20], sulfate end-groups are present and should undergo thermal depolymerization by unzipping from these poorly thermostable end-groups.

The second route of thermal degradation of PVDF occurs through the backbone scission, with the formation of halogenated or oxygenated compounds (e.g., $C_4H_3F_3$), monomer $(CH_2=CF_2)_n$, H–F and other alkyl radicals associated with high unsaturated residues [29, 30, 31]. This route is a practical case of homolytic scission, in which macroradicals are generated by scission of the covalent bonding between C–C atoms (bond strength of 348 kJ mol^{-1}) [4], and one electron remains attached to each fragment forming two free radicals.

In this work, the overall kinetics of the mass-loss process was investigated by TGA experiments at constant heating rates of 5, 10, 20, and 40 °C min^{-1}, as shown in Figure 6a, where thermal decomposition peak temperatures (T_{peak}) were also included (Figure 6b). It can be seen in Figure 6a that T_{onset} shifted to higher values when heating rate increases at the same conversion level, also shifting the DTG thermograms (Figure 6b), as expected, since that the material needs to absorb heat before its decomposition. Thus, if the heating rate increases, the material reaches higher decomposition temperatures indicating the methodology validity. Therefore, according to the formalism of the isoconversional method (OFW method), by plotting of ln β reciprocal $1/T$, the activation energy (E_a) of degradation process was obtained from the slope of resulting straight line. This is a critical evaluation since if E_a values remain the same at different conversion levels (α), it would indicate that the reaction takes place in a single step. On the other hand, changes in E_a with increasing of the aging/annealing time or degree of conversion may be indicative of the occurrence of more complex mechanisms during thermal degradation.

The OFW method was applied, and activation energies of PVDF were calculated according to Eq. (5) for different conversion levels during the thermal degradation process. The OFW plots for PVDF before and after aging in bioethanol and annealing during different experimental times are shown in Figure 7a—d. The values of activation energy, calculated for conversion levels in the range of $5 < \alpha < 50\%$, were obtained with correlation coefficients (R^2) above 0.9, indicating that the OFW method was successfully applied to the evaluation of thermal degradation kinetics of this PVDF. The activation energy values as a function of the extent of conversion level (α) are summarized in Table 3 and shown in Figure 8. Figure 7a—b shows different slopes for PVDF aged in bioethanol compared with those originated from the material annealed or unaged. These differences were more striking for the material aged in bioethanol for 90 days (Figure 7c). The non-parallel straight lines of Figure 7c indicated that there were changes in the initial activation energy of the thermal degradation process in this range of conversion, as can be conferred in the values summarized in Table 3. On the other hand, the material annealed (Figure 7d) presented an overall behavior similar to the value of unaged material. These results suggested a non-negligible influence of aging in bioethanol, differently from the effect of only annealing.

The average activation energy value of unaged PVDF, considering the range of $5 < \alpha < 50\%$, was ~185 kJ mol^{-1}, as shown in Table 3. This E_a value is compatible with literature reports [47, 73, 74] and remained approximately constant during thermal degradation in the range of temperature evaluated (Figure 8). After aging in bioethanol for 90 days, E_a suffered a reduction of 24%, and after 30 days of aging, although the profile of activation energy was less affected, the average E_a reached 11%

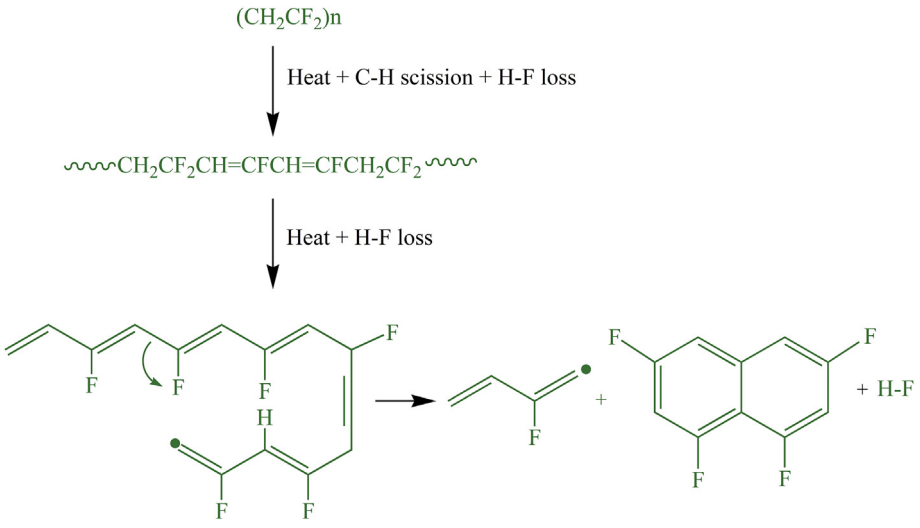

Figure 5. Reconstruction of the mechanism of H–F elimination followed by polyaromatization of PVDF during its thermal degradation. Elaborated based on [29, 30, 31, 32].

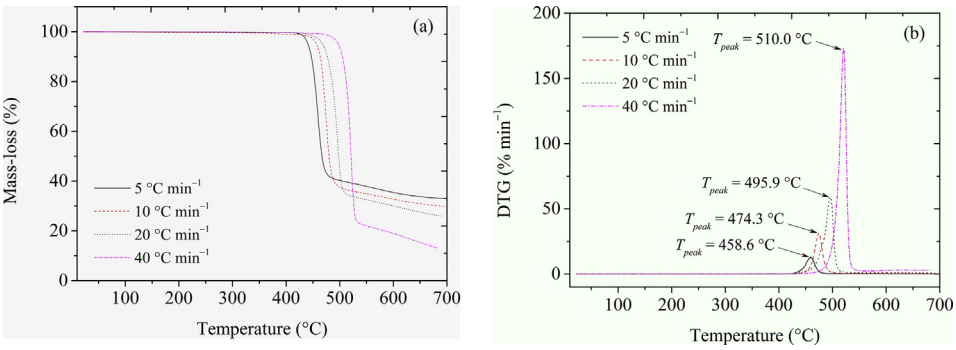

Figure 6. TGA (a), and DTG (b) thermograms of the unaged PVDF carried out at different heating rates.

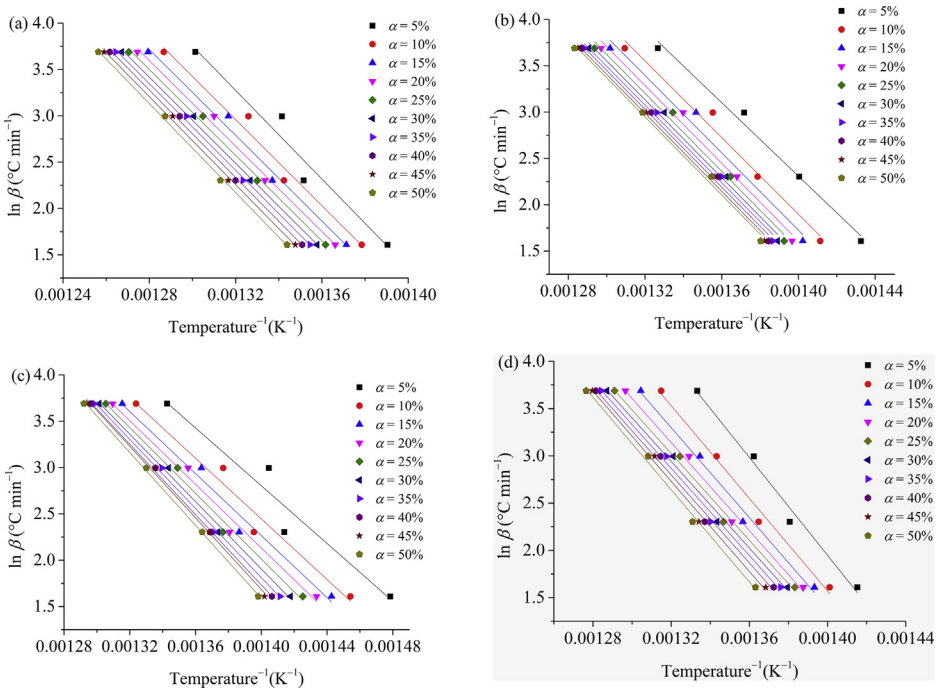

Figure 7. Ozawa-Flynn-Wall plot of isoconversional dynamic TGA data of PVDF in stages unaged (a), aged in bioethanol for 30 (b) and 90 (c) days, and annealed for 90 days (d).

Table 3. Activation energy values (E_a) and their respective conversion levels for PVDF in stages unaged, aged in bioethanol for 30 and 90 days and annealed for 90 days.

Conversion degree, α (%)	Unaged PVDF (kJ mol^{-1})	Aged 30 days in bioethanol (kJ mol^{-1})	Aged 90 days in bioethanol (kJ mol^{-1})	Annealed 90 days (sample 1) (kJ mol^{-1})	Annealed 90 days (sample 2) (kJ mol^{-1})
5	189.0	156.6	123.2	204.7	186.7
10	183.7	163.5	129.3	193.7	188.4
15	182.9	164.9	132.2	188.3	185.0
20	182.3	165.8	135.7	184.2	184.5
25	182.8	166.2	140.0	181.8	183.5
30	183.5	165.9	143.6	181.5	183.4
35	184.6	165.6	147.4	182.6	183.4
40	186.4	166.1	150.1	184.1	184.5
45	187.5	166.3	152.2	188.6	187.9
50	189.8	166.5	155.4	193.2	193.4
Average	185.3 ± 2.7	164.7 ± 3.0	140.9 ± 10.7	188.3 ± 7.3	186.1 ± 3.1

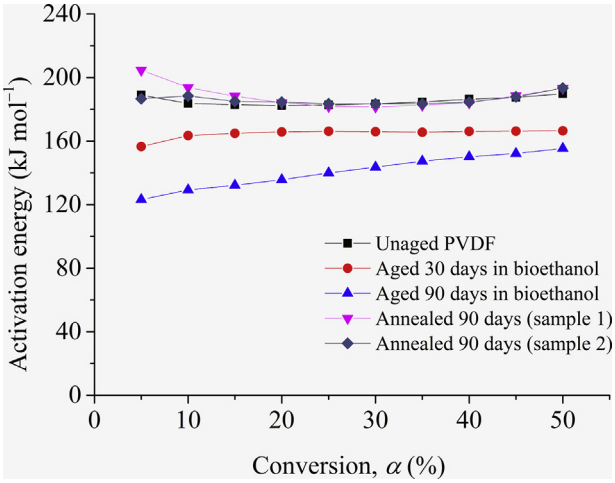

Figure 8. Dependence of activation energy as a function of the extent of conversion obtained from OFW method applied to thermal decomposition for PVDF in stages unaged, aged in bioethanol for 30 and 90 days, and annealed for 90 days.

of reduction. These reductions in E_a are attributed to the effect of bioethanol inside the free volume of PVDF amorphous structure, as related here, and also reported by us in [7], where it was shown that kinetics of fluid absorption tends to fit in the Fickian Case I diffusion behavior, i.e., the penetrant mobility is much lower than segmental relaxation rates. This result is in agreement with the small mass change variation founded for this PVDF in [7] (ca. 1.2 %, at nearly 90 days of immersion).

In the temperature range of ca. 400 — 500 °C, mass-loss was due to the main degradation process of PVDF, as shown in Figure 4a—b. Aging in bioethanol seems to favor this degradation, decreasing the activation energy for this process, i.e., the bioethanol acted catalyzing the PVDF thermal degradation. It was proposed that the mechanism predominant during the thermal degradation of PVDF was not the same after aging in bioethanol and after annealing. After annealing, it was supposed that the primary degradation followed the mechanism that was traditionally related [29, 30, 31, 32], i.e., occurred preferentially by C–H scission, with unzipping of H–F molecules down the polymer chain. In this case, the activation energy values were very close to the value of the unaged material, ca. 185 kJ mol^{-1}.

On the other hand, after aging in bioethanol, considerable differences in E_a values were observed. The initial step of bioethanol volatilization previously related seemed to favor the degradation. In this process, partial C–H scissions of bioethanol molecules also can contribute to the H–F eliminations in PVDF, increasing the number of radical specimens that reacts with H atoms, in a process that occurs by intra- or/and intermolecular H-transfers, as proposed by Schneider [75]. According to this author, after the intra- or/and intermolecular H-transfers, β-scissions may occur in vinyl polymers [75], leading to the formation of different chain fragments. Thus, due to the lower bond strength energy of C–C scissions (348 kJ mol^{-1}) [4] in β-scissions, the mean values of E_a were considerably less than those of unaged or annealed material, as shown in Table 3.

Figure 8 and Table 3 shows additionally that E_a values of PVDF aged in bioethanol for 30 and 90 days increased slightly with increasing conversion degree. This variation was an indication that different and simultaneous mechanisms took place after exposition in bioethanol and, consequently, energy may not always be constant, as indeed verified. Hence, the H-transfer process may have yielded different chain fragments of different lengths and volatilities, which are not necessarily volatiles at the temperature of their formation, changing the degradation temperature and E_a in the next conversion level.

When annealed PVDF was considered, the presence of bioethanol was nonexistent. Consequently, only minimal differences were verified in E_a values, as shown in Table 3. After 90 days of annealing, the increases in E_a were only 0.4 —1.6% (Table 3). This result indicated that the effect of only annealing using the temperature of 60 °C was minimum for this material, as expected since this polymer has a very high thermal stability. Concerning the relation between PVDF processing conditions and defect density with the thermal degradation kinetics, it has been reported that crystallinity and phase content was not relevant parameters for PVDF thermal degradation process [23, 29] since degradation occurs at high temperatures (more than 200 °C), in which the melted material has lost its thermal history.

On the other hand, the defect density parameter, given by amount of H–H and T-T configurations from ^{19}F and ^{2}H NMR spectroscopy [29, 76], respectively, was essential for the description of the polymer thermal degradation process. Hence, even though a moderate annealing temperature was used for this PVDF, secondary crystallization processes may occur, as reported for PVDF and other materials submitted to similar aging/annealing conditions [69, 77]. Consequently, a more homogeneous lamellae crystallites population was formed. This new structure, which was more concise due to a lower defect density, required consequently more energy to its overall thermal degradation, contributing to increasing the E_a values of PVDF annealed 90 days compared to the unaged one. However, since these were slight differences, the results indicated that annealing in the conditions evaluated did not play any role in the degradation process of this material, and consequently, limitations of the application were not verified.

3.4. Lifetime estimation

The Arrhenius activation energy values obtained using the OFW method were applied to construct the thermal endurance curves of PVDF before and after aging in bioethanol and after annealing by different experimental times. These curves were constructed according to the procedures of ASTM E1877 [38]. From these curves, the material lifetime was estimated for PVDF at different failure temperatures selected in the range of 25 up to 150 °C (temperatures in which PVDF is usually employed). It should be highlighted that, in practical cases, the lifetime might be variable, since in most real cases, multiple mechanisms can occur during the material decomposition with different dominant mechanisms in different ranges of temperature. In the present evaluation, a conversion degree of $\alpha = 10$ % was fixed, and the corresponding time in which this polymer was degraded was taken as the estimated thermal lifetime, also called time-to-failure of the material. Eq. (6) [38] was used for the thermal lifetime estimation.

$$\log t_f = \frac{E_a}{2.303RT_f} + \log\left(\frac{E_a}{R\beta}\right) - a \tag{6}$$

where E_a is Arrhenius activation energy (kJ mol^{-1}), R is universal constant (J mol^{-1} k^{-1}), β is heating rate nearest the midpoint of experimental heating rates, t_f is estimated thermal lifetime for a constant conversion level, which is taken as the failure criterion at a specific (or operation) failure temperature (T_f). Also, a is a tabulated numerical integration constant known as Doyle approximation [39, 41], which depends on both activation energy and temperature [39, 40, 41]. Figure 9 and Table 4 show the thermal lifetime behavior estimated for PVDF unaged, aged in bioethanol and annealed for different experimental times, which were obtained for different failure temperatures. From these results, it can be seen that both aging in bioethanol and thermo-aging (annealing) changed the material lifetime, but in different ways. While aging in bioethanol decreased lifetime at a fixed temperature, after annealing, the tendency is of lifetime increase, i.e., the effects were opposite.

The temperature needs to be moderated when PVDF is used as an inner layer of multilayer thermoplastic pipes or as a liner for steel pipelines or storage tanks, for example, keeping values below 60 °C for bioethanol storage or/and transportation [7, 15, 77, 78]. In the present study, considering the temperature of 25 °C, PVDF lifetime was 3.6 ×

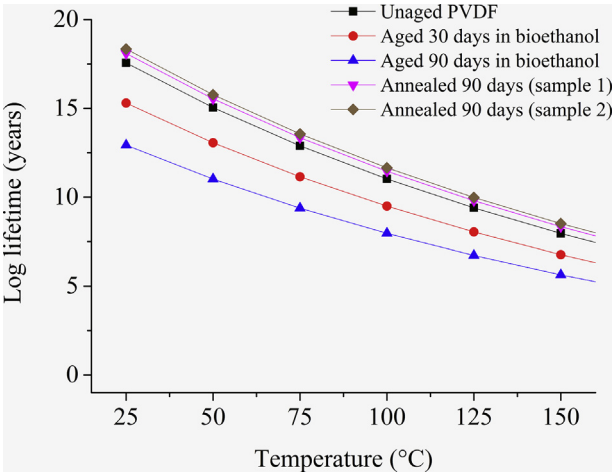

Figure 9. Thermal lifetime estimation for PVDF unaged and aged in bioethanol, and annealed by different times of exposition as obtained for different failure temperatures.

10^{17} years (Table 4), a very long time in the condition evaluated. After aging for 30 and 90 days in bioethanol at 25 °C, this value reduced to 2.0 × 10^{15} and 8.5 × 10^{12} years, respectively, indicating a not negligible effect of the fluid on material lifetime. Once that all these lifetimes were still quite elevated, the material can be used without any problem.

Besides, Figure 9 shows that the increase in temperature caused a sharp decrease in the lifetime of PVDF. Nevertheless, these variations were expected because the polymer lifetime was strongly dependent on the failure temperature selected. Hence, the increase in temperature tended to decrease material durability. For instance, when T_f changed from 25 to 60 °C, the lifetime of unaged material varied from 3.6 × 10^{17} to 1.4 × 10^{14} years; and after aging in bioethanol for 30 and 90 days at 60 °C, respective lifetimes reduced to 1.8 × 10^{12} and 2.1 × 10^{10} years, respectively, as shown in Table 4.

Comparing the estimated lifetime with the results obtained in [7], it can be observed that the different techniques indicated a very long lifetime, even with the significant differences in terms of magnitude of values. TGA/DTG thermograms revealed high stability for the material in biofuel, and an extensive lifetime even with reductions due to the effect of bioethanol. The general behavior revealed by TGA/DTG and DMTA [7] was corroborated between each other, indicating that these losses in durability were not enough to compromise the use of this material under the established conditions.

Differently from the PVDF aged in bioethanol, only annealing did not cause a reduction of the lifetime. On the contrary, those values increased slightly with annealing, as can be verified in Figure 9, in which thermal lifetime curves of two different samples of annealed PVDF were shifted up. In Figure 9, the lifetime of unaged material changed one decade after 90 days of annealing, considering T_f = 25 °C, i.e., 3.6 × 10^{17} to 1.2 × 10^{18} years for sample 1, and 2.2 × 10^{18} years for the sample 2 (Table 4). Likewise, considering annealing temperature of 60 °C, lifetime values of unaged PVDF varied from 1.4 × 10^{14} to 4.2 × 10^{14} (sample 1) and 7.0 × 10^{14} (sample 2), as also shown in Table 4. Moreover, the results indicate that, even when the material was exposed to very high temperature (130 °C), the lifetime was ca. 1.2 × 10^{9} years for unaged material and the values of 6.0 × 10^{7} and 3.1 × 10^{6} were achieved after aging of PVDF in bioethanol for times of 30 and 90 days (see Table 4), respectively. These overall results indicated that PVDF was an exceptionally durable material for this application, even if exposed to high temperatures such as 100 — 130 °C, and it showed that temperature played an active role in the overall material lifetime.

It is important to highlight that these TGA or DMTA [7] analyzes were carried out in an inert nitrogen atmosphere, and without considering any additional kind of mechanical, electrical, or environmental stress during aging. Therefore, it is believed that the material lifetime can be affected differently if another aging/annealing condition is considered.

Table 4. Thermal lifetime of PVDF in different conditions and times of exposition as obtained for different failure temperatures.

Unaged PVDF			
T_f (°C)	T_f (K)	t_f (years)	Log t_f (years)
25	298	3.6 × 10^{17}	17.6
60	333	1.4 × 10^{14}	14.1
130	403	1.2 × 10^{9}	9.1
Aged 30 days in bioethanol			
25	298	2.0 × 10^{15}	15.3
60	333	1.8 × 10^{12}	12.3
130	403	6.0 × 10^{7}	7.8
Aged 90 days in bioethanol			
25	298	8.5 × 10^{12}	12.9
60	333	2.1 × 10^{10}	10.3
130	403	3.1 × 10^{6}	6.5
Annealed 90 days (sample 1)			
25	298	1.2 × 10^{18}	18.1
60	333	4.2 × 10^{14}	14.6
130	403	6.3 × 10^{9}	9.8
Annealed 90 days (sample 2)			
25	298	2.2 × 10^{18}	18.3
60	333	7.0 × 10^{14}	14.8
130	403	9.7 × 10^{9}	10.0

4. Conclusions

The PVDF was prepared by compression molding and presented a mixture of α-, β- and γ-phases, α-phase as major contributor due to characteristics of the route of processing adopted. The appearance of β- and γ-phases, although unexpected, was confirmed and probably are correlated with the type of quenching applied.

For annealed PVDF, it was indicated that the primary degradation follows the mechanism traditionally related, i.e., occurs preferentially by C–H scissions followed by H–X elimination. After aging in bioethanol, thermal stability reduced, shifting the T_{onset} and T_{peak} towards lower values. It was supposed that bioethanol inside of the PVDF amorphous and constrained phases favors the primary step of thermal degradation through C–C scissions as a consequence of H-transfers followed by β-scissions of PVDF chains, producing a kind of catalyst effect on thermal degradation. Thus, lower values of E_a were obtained to PVDF samples aged in bioethanol compared to those unaged or annealed.

The overall results also showed that only annealing is not damaging to the material, unlike aging in bioethanol heated, where changes in the thermal degradation and lifetime were verified. These changes were associated with acting of PVDF β-phase that have active electric dipole moment similarly to the bioethanol.

By comparing the lifetime obtained from TGA/DTG and DMTA [7], it was observed that different methodologies indicated similar general behavior, i.e., high stability and an extensive lifetime, although with differences in terms of the magnitude of values. TGA/DTG indicated a decrease in the lifetime of PVDF after aging in bioethanol, similarly to the occurred with the long-term behavior observed through storage modulus master curves multiple frequencies from DMTA [7]. Even so, these changes are not enough to compromise the use of this material under the studied conditions because the material still presented exceptional durability. Therefore, it is suitable for applications at temperatures up to 60 °C in the presence of bioethanol, such as linings at storage tanks or multilayer pipelines.

Declarations

Author contribution statement

Agmar José de Jesus Silva: Conceived and designed the experiments; Performed the experiments; Analyzed and interpreted the data; Wrote the paper.

Maria Marjorie Contreras, Christine Rabello Nascimento: Analyzed and interpreted the data; Wrote the paper.

Marysilvia Ferreira da Costa: Conceived and designed the experiments; Analyzed and interpreted the data; Wrote the paper.

Funding statement

This work was supported by Agência Nacional de Petróleo, Gás Natural e Biocombustíveis — ANP (Grant PRH35—ANP), CAPES—PROEX (Grant 0113/2016) and CNPq (Grant 142160/2014-8).

Competing interest statement

The authors declare no conflict of interest.

Additional information

No additional information is available for this paper.

Acknowledgements

The authors thank CENPES/Petrobras SA and Solvay SA Company for supplying bioethanol fuel and PVDF, respectively.

References

[1] M. Kutz, Handbook of Environmental Degradation of Materials, William Andrew Publishing, New York, 2005.
[2] M. Abdallh, M. Bufaroosha, A. Ahmed, D.S. Ahmed, E. Yousif, Modification of poly(vinyl chloride) substrates via schiff's base for photochemical applications, J. Vinyl Addit. Technol. 26 (2020) 1–6.
[3] G.A. El-Hiti, D.S. Ahmed, E. Yousif, M.H. Alotaibi, H.A. Satar, A.A. Ahmed, Influence of polyphosphates on the physicochemical properties of poly(vinyl chloride) after irradiation with ultraviolet light, Polymers 12 (2020) 2–18.
[4] M. De Paoli, Degradação e Estabilização de Polímeros, Chemkeys, São Paulo, 2008.
[5] M. Alchikh, C. Fond, Y. Frère, H. Pelletier, Mechanochemical degradation of poly(vinyl fluoride) by sodium hydroxide measured by microindentation, J. Mater. Sci. 45 (2010) 2311–2316.
[6] J. Tarrío-Saavedra, J. López-Beceiro, A. Álvarez, S. Naya, S. Quintana-Pita, S. García-Pardo, F.J. García-Sabán, Lifetime estimation applying a kinetics model based on the generalized logistic function to biopolymers, J. Therm. Anal. Calorim. 122 (2015) 1203–1212.
[7] A.J. De Jesus-Silva, C.R. Nascimento, M.F. Costa, Thermomechanical properties and long-term behavior evaluation of poly(vinylidene fluoride) (PVDF) exposed to bioethanol fuel under heating, J. Mater. Sci. 51 (2016) 9074–9094.
[8] H. Teng, Overview of the development of the fluoropolymer industry, Appl. Sci. 2 (2012) 496–512.
[9] F.-C. Chiu, Y.-C. Chuang, S.-J. Liao, Y.-H. Chang, Comparison of PVDF/PVAc/GNP and PVDF/PVAc/CNT ternary nanocomposites: enhanced thermal/electrical properties and rigidity, Polym. Test. 65 (2018) 197–205.
[10] B. Yang, Y. Shi, J.-B. Miao, R. Xia, L.-F. Su, J.-S. Qian, P. Chen, Q.-L. Zhang, J.-W. Liu, Evaluation of rheological and thermal properties of polyvinylidene fluoride (PVDF)/graphene nanoplatelets (GNP) composites, Polym. Test. 67 (2018) 122–135.
[11] J.-L. Gacougnolle, S. Castagnet, M. Werth, Post-mortem analysis of failure in polyvinylidene fluoride pipes tested under constant pressure in the slow crack growth regime, Eng. Fail. Anal. 13 (2006) 96–109.
[12] F. Aquino, A. Stribeck, X. Li, A. Zeinolebadi, S. Buchner, G. Santoro, Variation of poly(vinylidene fluoride) morphology due to radial cold flow in a flexible pipe, Polym. Eng. Sci. 55 (2015) 2869–2877.
[13] S.A.E. Boyer, M. Gerland, S. Castagnet, Gas environment effect on cavitation damage in stretched polyvinylidene fluoride, Polym. Eng. Sci. 54 (2014) 2139–2416.
[14] M.M. Contreras, C.R. Nascimento, R.P. Cucinelli Neto, S. Teixeira, N. Berry, M.F. Costa, C.A. Costa, TD-NMR analysis of structural evolution in PVDF induced by stress relaxation, Polym. Test. 68 (2018) 153–159.
[15] K.J. Kallio, M.S. Hedenqvist, Ageing properties of polyamide-12 pipes exposed to fuels with and without ethanol, Polym. Degrad. Stabil. 93 (2008) 1846–1854.
[16] N. Messina, M. Mirenda, G. Besana, J.A. Abusleme, R. Faig, Process for Lining Metal Pipelines, 2014. US 2014/0083550 A1.
[17] M. Alchikh, C. Fond, Y. Frère, Discontinuous crack growth in poly(vinyl fluoride) by mechanochemical aging in sodium hydroxide, Polym. Degrad. Stabil. 95 (2010) 440–444.
[18] P. Kuyl, Y. Yamamoto, Dual-containment Pipe Containing Fluoropolymer, 2009. US 2009/0139596 A1.
[19] J.E. Mark, Polymer Data Handbook, Oxford University Press, New York, 2009.
[20] M.M. Contreras, C.R. Nascimento, R.P.C. Neto, S. Teixeira, N. Berry, M.F. Costa, C.A. Costa, Data on tensile tests and NMR measurements of poly(vinylidene fluoride) before and after stress relaxation, Data in Brief, Polym. Test. 19 (2018) 55–58.
[21] M. Frankel, Facility Piping Systems Handbook, McGraw-Hill, New York, 2009.
[22] M.L. Castelló, J. Dweck, D.A.G. Aranda, Kinetics study of thermal processing of glycerol by thermogravimetry, J. Therm. Anal. Calorim. 105 (2011) 737–746.
[23] S.F. Mendes, C.M. Costa, V. Sencadas, M. Pereira, A. Wu, P.M. Vilarinho, R. Gregorio, S. Lanceros-Méndez, Thermal degradation of Pb(Zr0.53Ti0.47)O3/poly(vinylidene fluoride) composites as a function of ceramic grain size and concentration, J. Therm. Anal. Calorim. 114 (2013) 757–763.
[24] S.F. Mendes, C.M. Costa, C. Caparros, V. Sencadas, S. Lanceros-Méndez, Effect of filler size and concentration on the structure and properties of poly(vinylidene fluoride)/$BaTiO_3$ nanocomposites, J. Mater. Sci. 47 (2012) 1378–1388.
[25] M. Jakić, N.S. Vrandečić, M. Erceg, Kinetics analysis of the non-isothermal degradation of poly(vinyl chloride)/poly(ethylene oxide) blends, J. Therm. Anal. Calorim. 123 (2016) 1513–1522.
[26] M.V. Kok, E. Topa, Thermal characterization and model-free kinetics of biodiesel sample, J. Therm. Anal. Calorim. 122 (2015) 955–961.
[27] P. Rajeshwari, Kinetics analysis of the non-isothermal degradation of high-density polyethylene filled with multi-wall carbon nanotubes, J. Therm. Anal. Calorim. 123 (2016) 1523–1544.
[28] C. Pətruţescu, G. Vlase, V. Turcuş, D. Ardelean, T. Vlase, P. Albu, TG/DTG/DTA data used for determining the kinetic parameters of the thermal degradation process of an immunosuppressive agent: mycophenolate mofetil, J. Therm. Anal. Calorim. 121 (2015) 983–988.
[29] G. Botelho, S. Lanceros-Méndez, A.M. Gonçalves, V. Sencadas, J.G. Rocha, Relationship between processing conditions, defects and thermal degradation of poly(vinylidene fluoride) in the β-phase, J. Non-Cryst. Solids 354 (2008) 72–78.
[30] S. Zulfiqar, M. Zulfiqar, M. Rizvi, A. Munirt, Study of the thermal degradation of polychlorotrifluoroethylene, poly(vinylidene fluoride) and copolymers of chlorotrifluoroethylene and vinylidene fluoride, Polym. Degrad. Stabil. 43 (1994) 423–430.

[31] G. Montaudo, C. Puglisi, E. Scamporrino, D. Vitalini, Correlation of thermal degradation mechanisms: polyacetylene and vinyl and vinylidene polymers, J. Polym. Sci. Part A Polym. Chem. 24 (1986) 301–316.

[32] M.L. O'Shea, C. Morterra, M.J.D. Low, Spectroscopic studies of carbons. XVII. Pyrolysis of polyvinylidene fluoride, Mater. Chem. Phys. 26 (1990) 193–205.

[33] ISO 175:2010, Plastics, Methods of Test for the Determination of the Effects of Immersion in Liquid Chemicals, British Standards Institution, 2010, pp. 1–32.

[34] C.H. Du, B.K. Zhu, Y.Y. Xu, Effects of stretching oncrystalline phase structure and morphology of hard elastic PVDF fibers, J. Appl. Polym. Sci. 104 (2007) 2254–2259.

[35] C.M. Costa, M.N.T. Machiavello, J.L.G. Ribelles, S. Lanceros-Méndez, Composition dependent physical properties of poly[(vinylidene fluoride)-co-trifluoroethylene]–poly(ethylene oxide) blends, J. Mater. Sci. 48 (2013) 3494–3504.

[36] D.W. Vankerselen, P.J. Hoftyzer, Properties of Polymers, Elsevier, Amsterdam, 1976.

[37] ASTM E1641, Standard test method for decomposition kinetics by thermogravimetry using the Ozawa/flynn/wall method, Annu. Book ASTM Stand. (2015) 1–7.

[38] ASTM E1877, Standard practice for calculating thermal endurance of materials from thermogravimetric decomposition data, Annu. Book ASTM Stand. (2009) 1–6.

[39] J.H. Flynn, L.A. Wall, A quick, direct method for the determination of activation energy from thermogravimetric data, J. Polym. Sci. B Polym. Lett. 4 (1966) 323–328.

[40] J.H. Flynn, L.A. Wall, Initial kinetics parameters from thermogravimetric rate and conversion data, J. Polym. Sci. B Polym. Lett. 5 (1967) 191–196.

[41] J.H. Flynn, L.A. Wall, General treatment of the thermogravimetry of polymers, J. Res. 70 (1966) 487–523.

[42] V.B. Carmona, R.M. Oliveira, W.T.L. Silva, L.H.C. Mattoso, J.M. Marconcini, Nanosilica from rice husk: extraction and characterization, Ind. Crop. Prod. 43 (2013) 291–296.

[43] V.B. Carmona, A. De Campos, J.M. Marconcini, L.H.C. Mattoso, Kinetics of thermal degradation applied to biocomposites with TPS, PCL and sisal fibers by non-isothermal procedures, J. Therm. Anal. Calorim. 115 (2013) 153–160.

[44] L.H. Gaabour, Thermal spectroscopy and kinetics studies of PEO/PVDF loaded by carbon nanotubes, J. Mater. 2015 (2015) 1–8.

[45] E. Turi, Thermal Characterization of Polymeric Materials, Academic Press, New York, 1981.

[46] Q. Ye, Z. Huang, Y. Hao, J. Wang, X. Yang, X. Fan, Kinetics study of thermal degradation of poly(l-lactide) filled with β-zeolite, J. Therm. Anal. Calorim. 124 (2016) 1471–1484.

[47] H. Li, H. Kim, Thermal degradation and kinetics analysis of PVDF/modified MMT nanocomposite membranes, Desalination 234 (2008) 9–15.

[48] P. Martins, A.C. Lopes, S. Lanceros-Méndez, Electroactive phases of poly(vinylidene fluoride): determination, processing and applications, Prog. Polym. Sci. 39 (2014) 683–706.

[49] J. Sun, L. Yao, Q.-L. Zhao, J. Huang, R. Song, Z. Ma, L.-H. He, W. Huang, Y.-M. Hao, Modification on crystallization of poly(vinylidene fluoride) (PVDF) by solvent extraction of poly (methyl methacrylate) (PMMA) in PVDF/PMMA blends, Front. Mater. Sci. 5 (2011) 388–400.

[50] Y. Bormashenko, R. Pogreb, O. Stanevsky, E. Bormashenko, Vibrational spectrum of PVDF and its interpretation, Polym. Test. 23 (2004) 791–796.

[51] L.C.M. Cirilo, M.F. Costa, Blends of PVDF with its processing waste: study of the mechanical properties of the blends thermally aged, in: M. Meyers, et al. (Eds.), Proceedings of the 3rd Pan American Materials Congress, the Minerals, Metals & Materials Series, Springer, Cham, 2017.

[52] T. Boccaccio, A. Bottino, G. Capannelli, P. Piaggio, Characterization of PVDF membranes by vibrational spectroscopy, J. Membr. Sci. 210 (2002) 315–329.

[53] Y. Liu, Y. Sun, F. Zeng, Y. Chen, Q. Li, B. Yu, W. Liu, Morphology, crystallization, thermal, and mechanical properties of poly(vinylidene fluoride) films filled with different concentrations of polyhedral oligomeric silsesquioxane, Polym. Eng. Sci. 53 (2013) 1364–1373.

[54] R. Gregorio, Determination of the α, β, and γ crystalline phases of poly(vinylidene fluoride) films prepared at different conditions, J. Appl. Polym. Sci. 100 (2006) 3272–3279.

[55] B. Mohammadi, A.A. Yousefi, S.M. Bellah, Effect of tensile strain rate and elongation on crystalline structure and piezoelectric properties of PVDF thin films, Polym. Test. 26 (2007) 42–50.

[56] R. Song, D. Yang, L. He, Effect of surface modification of nanosilica on crystallization, thermal and mechanical properties of poly(vinylidene fluoride), J. Mater. Sci. 42 (2007) 8408–8417.

[57] C.-L. Liang, Q. Xie, R.-Y. Bao, W. Yang, B.-H. Xie, M.-B. Yang, Induced formation of polar phases in poly(vinylidene fluoride) by cetyl trimethyl ammonium bromide, J. Mater. Sci. 49 (2014) 4171–4179.

[58] V. Sencadas, C.M. Costa, J.L. Gómez Ribelles, S. Lanceros-Méndez, Isothermal crystallization kinetics of poly(vinylidene fluoride) in the α-phase in the scope of the Avrami equation, J. Mater. Sci. 45 (2009) 1328–1333.

[59] A.B. Da Silva, C. Wisniewski, J.V.A. Esteves, R. Gregorio, Effect of drawing on the dielectric properties and polarization of pressed solution cast β-PVDF films, J. Mater. Sci. 45 (2010) 4206–4215.

[60] M. Inoue, Y. Tada, K. Suganuma, H. Ishiguro, Thermal stability of poly(vinylidene fluoride) films pre-annealed at various temperatures, Polym. Degrad. Stabil. 92 (2007) 1833–1840.

[61] C. Ribeiro, C.M. Costa, D.M. Correia, J. Nunes-Pereira, J. Oliveira, P. Martins, R. Gonçalves, V.F. Cardoso, S. Lanceros-Méndez, Electroactive poly(vinylidene fluoride)-based structures for advanced applications, Nat. Protoc. 13 (2018) 681–704.

[62] D. Song, D. Yang, Z. Feng, Formation of β-phase microcrystals from the melt of PVF_2-PMMA blends induced by quenching, J. Mater. Sci. 25 (1990) 57–64.

[63] T. Hattori, M. Hikosaka, H. Ohigashi, The crystallization behaviour and phase diagram of extended-chain crystals of poly(vinylidene fluoride) under high pressure, Polymer 37 (1996) 85–91.

[64] W.W. Doll, J.B. Lando, Polymorphism of poly(vinylidene fluoride). 3.Crystal structure of phase-II, J. Macromol. Sci. Part B. 4 (1970) 309–329.

[65] W.W. Doll, J.B. Lando, Polymorphism of poly(vinylidene fluoride). 4. Structure of high-pressure-crystallized poly(vinylidene fluoride), J. Macromol. Sci. Part B. 4 (1970) 889–896.

[66] T. Hattori, M. Kanaoka, H. Ohigashi, Improved piezoelectricity in thick lamellar beta-form crystals of poly(vinylidene fluoride) crystallized under high pressure, J. Appl. Phys. 79 (1996) 2016–2022.

[67] D. Yang, Y. Chen, Beta-phase formation of poly(vinylidene fluoride) from the melt induced by quenching, J. Mater. Sci. Lett. 6 (1987) 599–603.

[68] Y. Oka, N. Koizumi, in: Formation of Unoriented Form I Poly(vinylidene Fluoride) by High-Rate Quenching and its Electrical Properties, 63, Bulletin of the Institute for Chemical Research, Kyoto University, 1985, pp. 192–206.

[69] S. Castagnet, D. Girard, Sensitivity of damage to microstructure evolution occurring during long-term high-temperature annealing in a semi-crystalline polymer, J. Mater. Sci. 42 (2007) 7850–7860.

[70] Z.-Y. Wang, H.-Q. Fan, K.-H. Su, Z.-Y. Wen, Structure and piezoelectric properties of poly(vinylidene fluoride) studied by density functional theory, Polymer 47 (2006) 7988–7996.

[71] W. Li, B. Sun, P. Wu, Study on hydrogen bonds of carboxymethylcellulose sodium film with two-dimensional correlation infrared spectroscopy, Carbohydr. Polym. 78 (2009) 454–461.

[72] S. Mitra, A. Ghanbari-Siahkali, P. Kingshott, S. Hvilsted, K. Almdal, Chemical degradation of an uncrosslinked pure fluororubber in an alkaline environment, J. Polym. Sci., Part A: Polym. Chem. 42 (2004) 6216–6229.

[73] Z.-W. Ouyang, E.-C. Chen, T.-M. Wu, Thermal stability and magnetic properties of polyvinylidene fluoride/magnetite nanocomposites, Materials 8 (2015) 4553–4564.

[74] M.N. Wadekar, Y.R. Patil, B. Ameduri, Superior thermostability and hydrophobicity of poly(vinylidene fluoride-co-fluoroalkyl 2-trifluoromethacrylate), Macromolecules 47 (2014) 13–25.

[75] H.A. Schneider, The quantitative evaluation of TG-curves of polymers, Thermochim. Acta 83 (1985) 59–70.

[76] E. Katoh, K. Ogura, I. Ando, An NMR study of poly(vinylidene fluoride) structure by ^{1}H, ^{13}C, and ^{19}F triple resonance method, Polym. J. 26 (1994) 1352–1359.

[77] A.J. De Jesus-Silva, N.G. Berry, M.F. Costa, Structural and thermo-mechanical evaluation of two engineering thermoplastic polymers in contact with ethanol fuel from sugarcane, Mater. Res. 19 (2016) 84–97.

[78] A.J. De Jesus-Silva, M.F. Costa, Mechanical evaluation of polymeric materials using instrumented indentation technique: concepts review and case study, Rev. Eng. Tecnol. 11 (2019) 212–224.